http://dx.doi.org/10.2106/JBJS.16.01321

Appendix

Specimen Preparation

The specimens (obtained from donors who were an average of 84 ± 2 years old at the time of death) were thawed at room temperature overnight prior to the experiment. None of the specimens had a flexion contracture of >10°, a pronation-supination rotation arc of <140°, or radiographic evidence of arthritis or deformity. The skin and subcutaneous fat were removed from the midpart of the humerus to 5 cm distal to the elbow joint. The biceps, brachialis, and triceps muscle bellies were removed while their tendon insertions were preserved and prepared with locking Krackow stitches using a 36-kg (80-lb)-test braided Dacron (synthetic polyester fiber; duPont) fishing line. The humeral origins of the flexor pronator and extensor supinator muscles were preserved. To permit placement of the pressure transducer while minimizing the wrinkles therein, the anterior aspect of the capsule was excised, taking care not to injure the collateral or annular ligaments. Any specimen with cartilage erosion to the subchondral bone was excluded, but we did not discard specimens exhibiting shallow erosion with fibrillation and fissuring with normal joint contact. Any specimen with ligament insufficiency (detected either by performing the posterolateral rotatory drawer test[26] or with direct visualization of the ligaments) was excluded. The proximal humeral end of the specimen was then potted into a cylindrical metal sleeve in parallel to its long axis using polyurethane resin (Smooth-Cast 65D; Techno-Industrial Products) to fix and load the specimen onto the testing machine[27].

Pressure Transducer

A Tekscan 5051 thin-film pressure transducer with a saturation pressure of 8.3 MPa (1,200 psi) was laminated with 2 layers of thin plastic to protect it, to prevent it from wrinkling in the joint, and to allow the placement of 4 lines that were sutured to the edge of the plastic fold without damaging the sensor. These lines, which were inserted through the joint from anterior to posterior by using a needle, helped us to pull the sensor into the joint. Then, the lines were secured to a 3.5-mm olecranon LCP plate (AO Synthes), used to fix the osteotomy site, to prevent the sensor from changing its position on the ulnar joint surface and from eventually exiting the joint. With use of this approach, the sensor moved along with the ulna on the humeral surface during the flexion motion and consistently showed the contact area and pressure of the same portion of the joint. Rigid fixation of the olecranon osteotomy site prevented macroscopic movements across that site.

The thin-film Tekscan sensor has been validated for rounded contact areas[28] and was used in earlier studies of joint contact pressures at multiple areas of contact[29,30]. It was recently used to study contact pressures in the elbow joint[27]. Each 5051 sensor has one 56 × 56-mm matrix, comprising 1,936 sensels (individual 0.8 × 0.8-mm pressure detection units of the pressure sensor) located on conductive ink grids.

As previously performed by other authors, the sensor was calibrated each and every time prior to being inserted in the elbow joint[27,31,32]. The sensor's calibration was performed with the Tekscan I-Scan software using an MTS machine (model 312, MTS Systems) to apply 8 sequential loads to the sensor while it was sandwiched between 2 layers of 1.6-mm rubber membrane, which was in turn sandwiched between 2 polished aluminum plates. The calibration pressure loads ranged from 690 to 5,520 kPa (100 to 800 psi) and were applied in 690-kPa (100-psi) increments. Since it is recommended that sensors be calibrated under conditions that mimic

those encountered during testing[24], the membrane-aluminum calibration construct was chosen to mimic the cartilage-subchondral bone conditions of the elbow joint. The Tekscan data were captured at a frequency of 100 Hz. Once this calibration was completed, these angle data, captured at 100 Hz, allowed us to accurately calculate and compare the angular speeds of flexion throughout the forearm arc of motion.

Specimen Mounting, Motion Simulation, and Flexion/Extension Angle Detection

The specimen was then mounted on a custom-made machine (Fig. 1) designed to test the elbow while it was passively flexed from 0° to 90° at various degrees of humeral internal rotation. The biceps, brachialis, and triceps were connected, using cords passing through pulleys (Fig. 1, gray pulleys), to Airpel pneumatic pistons (Airpot) to simulate muscle loads with the aim of providing dynamic joint stability. The distance of each pulley from the joint line and from the humeral axis was set in an extended neutral position to simulate the physiologic position of the tendons[33] 5.5 cm proximal to the joint line. The brachialis, biceps, and triceps pulleys were set at 2, 3.5, and 2 cm away from the humeral axis, respectively. The elbow was passively flexed by pulling a braided Dacron line perpendicularly to the forearm throughout the range of motion to avoid the stabilizing/distracting effect of an external force[34]. The pronated position naturally assumed by the forearm when the humerus is internally rotated was maintained by avoiding any torque on the wrist or forearm. To collect the angle data throughout the range of motion, a line held in tension by a 130-g weight was connected to the volar aspect of the ulna 20 cm distal to the elbow joint and passed through a pulley (Fig. 1, white pulley) connected to a potentiometer. The excursion of the line over the white pulley during the elbow flexion arc generated a voltage output that was captured simultaneously with the Tekscan data in real time at 100 Hz and converted to flexion angle data using a custom LabVIEW software (National Instruments) virtual instrument (VI). This voltage-angle conversion was uniquely calibrated for each specimen using a goniometer to generate a 10-point standard curve to accommodate the different forearm lengths encountered in each specimen. The R^2 for the standard curves was always >0.99.

Testing Protocol

To reduce the friction between the joint surface and the sensor, 2 mL of mineral oil (Sigma-Aldrich) was applied to the joint after sensor insertion. The articular surfaces and the tendons were frequently moistened with normal saline solution during testing. Specimens were mounted such that the humerus was placed in a position corresponding to 90° of forward flexion (i.e., rotation in the sagittal plane) from the anatomic position. We refer to this position as 0° of humeral rotation, and from there the humerus was internally rotated varying amounts up to 90°. The intact elbows were tested in 3 different degrees of humeral internal rotation: 15°, 45°, and 90°. At each angle of humeral rotation, the elbow was flexed with 1 continuous movement from 0° to 90° 6 different times with increasing loads on the brachialis, biceps, and triceps tendons. Although the loads were changed, the ratio of loads was maintained as 1:1:2 for the brachialis, biceps, and triceps, respectively, as previously reported[35-38]. From 10, 10, and 20 N (applied to the brachialis, biceps, and triceps tendons, respectively), we progressively increased the forces to 35, 35, and 70 N in increments of 5, 5, and 10 N, respectively. These intact-elbow data were collected at these various muscle loads to ensure that appropriate control data were available for comparison with those data obtained at the minimum muscle loads at which the PMRI elbows experienced the shift from subluxation to reduction (described in greater detail below).

Then, after removing the sensor (to allow proper joint visualization), a PMRI injury was simulated (PMRI elbows). The posterior bundle of the MCL was sectioned from the posterior margin of the olecranon to the non-articular bare area of the ulna, as was previously described by Pollock et al.[10]. An LCL tear was created in such a way as to mimic the pathology seen in elbows with acute PMRI in which the LCL is avulsed from the humeral epicondyle and retracted underneath the extensor tendon from which it delaminates. To do this, the LCL was exposed through the anterior capsulectomy, dissected from the undersurface of the extensor tendons, and cut at the joint line, without affecting the integrity of the tendons. A positive posterolateral rotatory drawer test[26] confirmed the lesion to be adequate. Finally, based on a technique developed in a pilot study, an anteromedial subtype-2 coronoid fracture[1] was created (Fig. E1).

http://dx.doi.org/10.2106/JBJS.16.01321

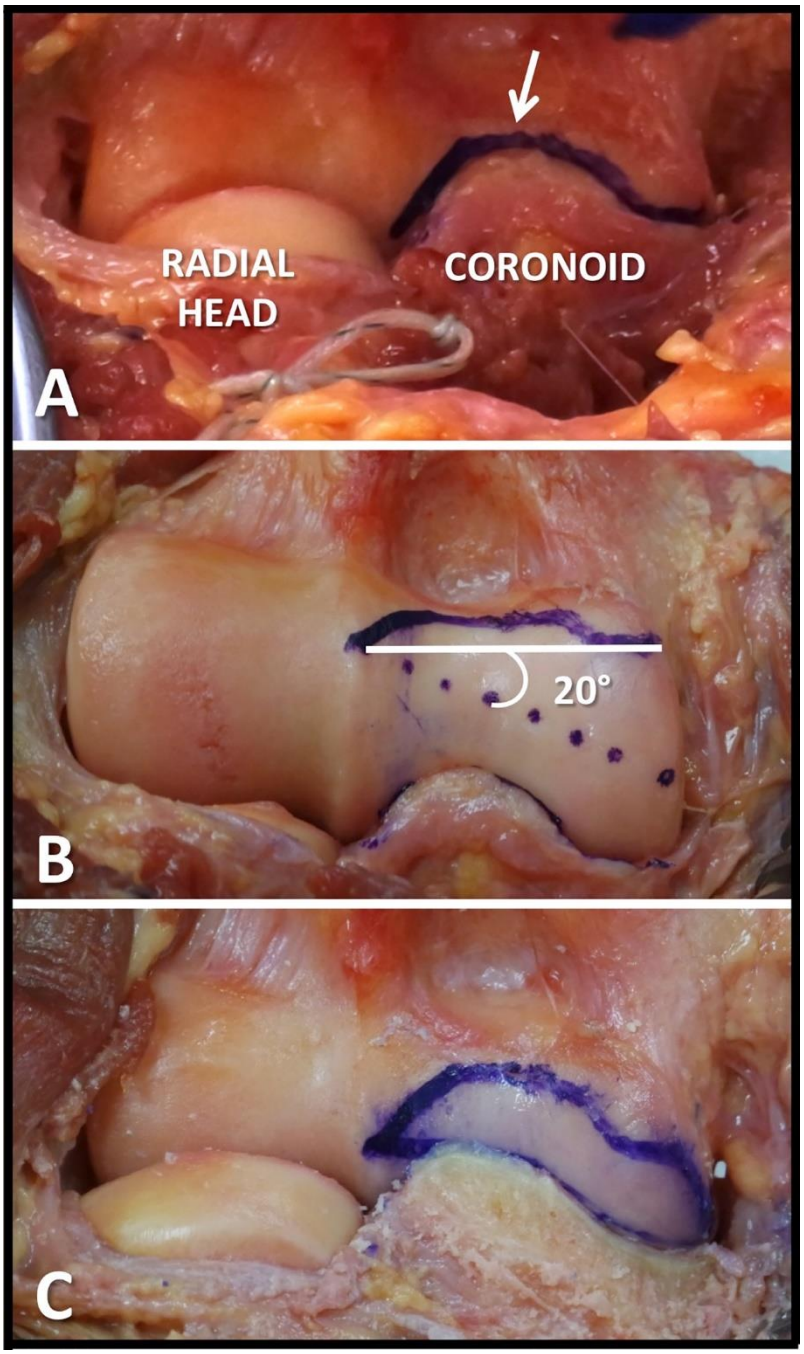

Fig. E1

Figs. E1-A, E1-B, and E1-C Preparation of the anteromedial subtype-2 coronoid fracture. (By permission of Mayo Foundation for Medical Education and Research. All rights reserved.) **Fig. E1-A** With the elbow at 90° of flexion, the coronoid margin was outlined on the trochlear surface (white arrow) from the trochlear ridge to the medial trochlear edge. **Fig. E1-B** With the elbow in full extension, a dotted line was drawn from the trochlear ridge toward the medial edge of the trochlea, with 20° of tilt with respect to the horizontal plane (white line), between the trochlear ridge and the marking previously made at the medial trochlear edge. **Fig. E1-C** With the elbow in 90° of flexion, the coronoid osteotomy was performed from anterior to posterior and refined with a high-speed burr until the osteotomy matched the dotted line on the trochlear surface.

Then, the PMRI elbows were tested, without the sensor, at 15°, 45°, and 90° of humeral internal rotation to detect the first flexion angle value at which the elbow reduced (reduction angle). We started testing with the first pattern of load (as described above for the intact elbow), and we progressively increased the tendon loads until reduction was seen. This was done in order to determine the minimum muscle loads at which the elbows experienced the shift from subluxation to reduction. In fact, a pilot study showed that, in larger specimens, a low force can sometimes be insufficient to permit the subluxation to reduce (presumably due to the greater forearm mass). The same procedure was then performed after the insertion of the sensor since a pilot study showed that the load at which the reduction can be detected can differ according to whether the sensor is or is not in place (i.e., the reduction load was usually lower without the sensor). We surmised that this was due to the sensor covering the sharp osseous edge of the fracture, thus making the spontaneous reduction less prominent. Since the repetitive shift from subluxation to reduction was observed to wear out the sensor prematurely, a worn-out sensor was placed in the joint while the appropriate testing load was being determined. Then, the PMRI elbows were tested with a fresh sensor at 15°, 45°, and 90° of humeral internal rotation only under the loading condition previously determined with the worn-out sensor. Hence, the data collected for the PMRI elbow were finally compared only with the previously collected intact-elbow data under the same loading condition. For example, if the appropriate data acquisition for the PMRI elbow was found to be at testing loads of 25, 25, and 50 N (in the biceps, brachialis, and triceps, respectively), the intact control data were considered to be those data collected in the intact elbow also at testing loads of 25, 25, and 50 N.

Data Measurements

Data were recorded at 100 Hz using the Tekscan software (I-Scan). Contact pressure, contact area, and the center of force on the coronoid were calculated, rounded to 2 significant digits of accuracy, and presented as the mean and standard error of the mean. The center-of-force result, the position on the joint surface that illustrates the balance of forces acting across the joint, was also calculated using the Tekscan software at all flexion angles.

To minimize the risk of collecting spurious joint-contact data, before every testing session we registered landmarks with a metal probe on the actual ulnar joint surface covered by the sensor and mapped them to the sensor in real time on the computer display. Doing so permitted us to confirm that any wrinkle-related contact artifacts were present only outside the joint areas being measured. These landmarks also guided us in drawing the polygons using the I-Scan software to consistently collect only the relevant contact pressure and area data regardless of minor sensor-position changes that resulted from the removal and reinsertion of the sensor between tests. Moreover, while drawing the polygons, we omitted the 4 lines of sensels closest to the olecranon osteotomy where the sensor was always pinched.

The points corresponding to the beginning of elbow reduction (pre-reduction point) and the completion of reduction (post-reduction point) were determined by watching videos recorded and synchronized with the Tekscan and flexion-angle-data acquisition streams. A video camera pointed right at the medial aspect of the elbow joint was used.

Statistical Analysis

All raw data (i.e., the data set comprising the output from each Tekscan sensel) were filtered using a 4th-order, low-pass Butterworth filter with a 50-Hz cutoff frequency. Data were

then down-sampled using spline interpolation. This involved generating a curve from the thousands of data points in each test and, from that curve, determining discrete angle values from 0° to 90° in 1-integer increments, which was necessary to perform discrete data analysis. To obtain an average curve for each group, the contact pressures and areas corresponding to each discrete angle from all of the specimens in that group were similarly analyzed. To ensure that the down-sampling process did not significantly affect the outcome measures, the R^2 correlation of the filtered and down-sampled data were confirmed to be ≥0.98. The data were modeled using analysis of variance (ANOVA) with $p < 0.05$ considered to be significant. All data were analyzed using 1 or 2-factor repeated-measures ANOVA with least squares means-contrast post hoc comparisons and Bonferroni corrections where appropriate. P values of <0.05 were considered to be significant. Comparisons between the intact and PMRI elbows were made at the angles corresponding to the pre-reduction and post-reduction points for each specimen.

Power calculations for the 7 specimens that were ultimately used in our analysis revealed that, with $\alpha = 0.05$, we had at least an 80% chance of detecting a significant difference of 1.3 standard deviations. In the context of our repeated-measures analyses, this meant that, in the PMRI-elbow group for example, we had an 80% chance of detecting a significant difference in area of 55 mm^2 and a significant difference in pressure of 205 kPa between the pre-reduction and post-reduction points.

Center-of-Force Results

The mean length of the center-of-force-path segment during the elbow reduction (i.e., from point "b" to "c" in Figure 5) was 7 ± 1 mm, which was significantly greater than the center-of-force path length of the intact elbows during the same range of flexion (3 ± 1 mm) ($p = 0.01$). No significant effect of humeral internal rotation on the center-of-force-path length ($p \geq 0.52$) or the time required for the center of force to complete its path ($p \geq 0.75$) was observed.

At each humeral internal rotation position, the velocity of movement of the center of force during reduction in the PMRI elbows was significantly higher than the speed of the center of force in the intact elbows during the corresponding range of flexion ($p = 0.002$). Compared with the mean speed of the center of force from 0° to 90° in the intact elbows, the mean speed during the elbow reduction (in the PMRI elbows) was increased by a mean of 440% ± 125% at 15° of humeral internal rotation, 535% ± 135% at 45° of humeral internal rotation, and 370% ± 120% at 90° of humeral internal rotation. The degree of humeral internal rotation had a significant effect on the center-of-force velocity ($p = 0.006$).

Contact Areas and Pressures According to Location on Coronoid

In the PMRI elbows, contact was principally on the medial aspect of the coronoid in full extension. As the severity of elbow subluxation increased during flexion, contact was concentrated near the fracture edge on the anteromedial aspect of the coronoid (red and green lines, respectively, in Figs. 6-A and 6-B). During elbow reduction, the contact area dramatically increased due to improved contact with the posterior aspect of the coronoid (Fig. 6-A, blue line), but also due to contact with more of the medial aspect of the coronoid (Fig. 6-B, green line), and not just near the fracture edge. This was more evident at 15° of humeral internal rotation.

Contact pressures in the PMRI elbows were much higher on the anteromedial aspect of the coronoid initially (red and green lines, respectively, in Figs. 6-C and 6-D). With progressive elbow subluxation during flexion, contact pressures increased on the lateral aspect of the coronoid (Fig. 6-D, pink line). The elbow reduction was accompanied by a dramatic decrease in pressure on the anterior aspect of the coronoid (Fig. 6-C, red line), both medially and laterally. There was a slight increase in pressure on the posterior aspect of the coronoid (Fig. 6-C, blue line) as it began to articulate with the trochlea. Contact with the lateral aspect of the coronoid changed quite substantially, increasing during progressive subluxation and then dropping suddenly during elbow reduction (Fig. 6-D, pink line).